RSC Advances

PAPER

View Article Online
View Journal | View Issue

Cite this: *RSC Adv.*, 2024, **14**, 34556

Functionalized porous carbon microspheres packed column for solid phase extraction and preconcentration of trace metal ions in food and water samples

Syed Ghazanfar Ali,[a] Sakshi Kapoor,[b] Rais Ahmad Khan,[c] Uzma Haseen *[d] and Haris Manzoor Khan[a]

Porous materials play a crucial role in the extraction of trace analytes; yet, the attainment of high selectivity and efficient regeneration continues to pose a considerable problem. In this study, we employed a green method to synthesize porous carbon microspheres. These microspheres were subsequently functionalized with aminophosphonic acid to facilitate the extraction of heavy metal ions from real samples. A comprehensive analysis of the aminomethylphosphorylated carbon microspheres was conducted using FTIR, SEM, EDX, TEM, BET and water contact angle measuring techniques. The potential optimization of analyte enrichment can be accomplished by the proposed solid-phase extraction (SPE) approach, which notably reduces spectrum interferences following sample purification. Following the IUPAC equation, the detection limit of the proposed method was found to be 0.04 ng mL^{-1}, after running 20 replicate blank tests. The primary focus of sequestration of trace metal ions is the formation of metal–ligand chelates within the carbon spheres, resulting in enhanced selectivity and extraction rates exceeding 99.9% from samples with low concentrations. The present studies show a significant preconcentration limit of 0.4 ng mL^{-1} and a substantial preconcentration factor of 500. The method was implemented to examine real food and water samples, and the obtained data exhibit significant accuracy with a relative standard deviation (RSD) of less than 5%.

Received 24th August 2024
Accepted 20th October 2024

DOI: 10.1039/d4ra06137c

rsc.li/rsc-advances

1. Introduction

Over the past few decades, there has been a significant focus within the scientific community on the issue of heavy metal pollution, primarily due to its adverse effects on living biota.[1–3] The escalating levels and ubiquitous nature of heavy metals in industrial discharges, wastewater, and contaminated soils pose serious threats to ecosystems and human health.[4–6] This increased awareness highlights the urgent requirement for effective strategies to mitigate contamination and protect human health.[7,8] Conventional approaches such as chemical precipitation, ion exchange, and adsorption have been extensively utilized methods for the removal of heavy metals, especially in situations involving high metal concentrations.[9] Nevertheless, their effectiveness significantly diminishes when addressing scenarios of trace-level heavy metal removal and often falls short in terms of efficiency, selectivity, and environmental sustainability.[10–12] As a result, the development of efficient and versatile materials capable of effective removal of heavy metals at low concentrations is necessary. Importantly this can be achieved by increasing the interaction and accessibility of metal ions towards the binding sites of developed materials.[13]

A highly promising alternative strategy involves the utilization of micro/nanoscale adsorbents, which have demonstrated significant potential in achieving the reduction of metal concentrations to trace levels. Various new materials, including metal oxide nanoparticles,[14,15] graphene oxide,[16] metal–organic frameworks,[17,18] and several other nano-sorbents,[19,20] have been explored for their metal sequestration. However, porosity remains a challenge in these materials; most of them have low porosity and are not very effective in the remediation of heavy metals at trace level concentrations.

The advent of carbon microspheres represents a breakthrough in the quest for innovative materials that can simultaneously address these limitations.[21] Porous carbon

[a]*Department of Microbiology, Jawaharlal Nehru Medical College, Aligarh Muslim University, Aligarh-202002, U.P, India*

[b]*Nanoscale Research Facility, Indian Institute of Technology Delhi, Hauz Khas, New Delhi-110016, India*

[c]*Department of Chemistry, College of Science, King Saud University, Riyadh 11451, Saudi Arabia*

[d]*Department of Chemistry, Aligarh Muslim University, Aligarh-202002, U.P, India. E-mail: uzmahaseen.chem@gmail.com*

Table 1 Comparison of SPE parameters of FCM with other existing methods

Sorbent	Capacity (mg g^{-1})	Preconcentration factor	Preconcentration limit (ppb)	Detection limit (ppb)	Ref.
FCM	373-Pb(II) 247-Cd(II)	500-Pb(II) 500-Cd(II)	0.4-Pb(II) 0.4-Cd(II)	0.04-Pb(II) 0.04-Cd(II)	This work
PHBvbNCl	175-Pb(II) 153-Cd(II)	114-Pb(II) 98-Cd(II)	—	0.03-Pb(II) 0.15-Cd(II)	26
Fe3O4 @UiO-66-SH	—	—	—	0.17-Pb(II) 0.21-Cd(II)	27
Cellulose nitrate	—	100-Pb(II) 125-Cd(II)	—	0.1–0.7	28
Graphene oxide	—	400-Pb(II) 200-Cd(II)	—	0.05-Pb(II) 0.05-Cd(II)	29
GO-AAO	—	700-Pb(II) 700-Cd(II)	1.4-Pb(II) 1.4-Cd(II)	1.2-Pb(II) 1.2-Cd(II)	12

microspheres have garnered considerable attention as promising candidates for addressing this challenge due to their unique structural characteristics and diverse surface functionalities.[22] This class of materials holds immense potential in the realms of heavy metal sequestration and analysis, offering a synergistic combination of adsorption capabilities, high surface area, and tunable surface chemistry. By integrating porous structures with tailored carbonaceous compositions, these microspheres exhibit superior adsorption capacities and selective binding affinities towards various heavy metal ions at trace level concentration.[23] Moreover, the multifunctionality of these carbon microspheres extends beyond their sequestration capabilities. Their surface can be modified to incorporate specific functional groups, enabling the design of materials with enhanced selectivity and adaptability for targeted heavy metal removal.[24,25] Additionally, the porous architecture facilitates efficient mass transfer, ensuring rapid adsorption kinetics and improved overall performance. A comparative analysis of developed sorbent and previous reported materials has been compared and presented in Table 1.

This work delves into the synthesis, functionalization, and applications of porous carbon microspheres as efficient material for heavy metal sequestration and analysis. By examining the underlying principles governing their design and performance, this study aims to contribute valuable insights into the development of sustainable and effective solutions for mitigating the adverse impacts of heavy metal contamination on the environment and public health. As the demand for innovative environmental technologies continues to grow, the exploration of mesoporous multifunctional carbon microspheres stands poised at the forefront of scientific advancements in the field of environmental remediation and analytical chemistry.

2. Materials and methods

2.1. Reagents

Sucrose ($C_{12}H_{22}O_{11}$, 98.5%), ethanol (C_2H_5OH, 99%), polyaminophosphonic acid (poly-($NH_2C_2H_5P(O)(OH)_2$, 99%) and metal salts were purchased from Sigma Aldrich and used without further purification. Deionized water (18 MΩ cm) was used to prepare all solutions.

2.2. Synthesis of carbon microspheres (CM)

The synthesis of porous CM was carried out by hydrothermal polymerization and emulsification of sucrose.[22] To do this, a 130.0 g of sucrose were dissolved in 250 mL of deionized water and sealed in a Teflon autoclave for 2 h at 200 °C. After cooling down to room temperature, the brown suspension of porous CM was collected and repeatedly cleaned with ethanol and water. After 12 h of vacuum drying at 60 °C, the final CM material was placed in a desiccator before further functionalization. The successful formation of highly porous structures relies on the use of robust conjugated polymeric precursors, which facilitate the development of an adequate carbon framework and maintain structural integrity under hydrothermal conditions, even when subjected to elevated thermal environments. The resulting composite material (CM) displays a well-defined spherical morphology with a narrow particle size distribution. The observed slight variation in CM size may be attributed to framework shrinkage occurring during the hydrothermal process, which was conducted without the use of a template.

2.3. Functionalization of CM

In first step, 2.0 g of the as-synthesized CM was dispersed under bath sonication in 50 mL of the C_2H_5OH/H_2O (1 : 1) solution containing diluted 0.5 g of polyaminophosphonic acid. The whole reaction suspension was sonicated for 30 min to diffuse the ligand inside the porous CM. The reaction solution was refluxed for 6 h under constant stirring at 60 °C. The obtained product (FCM) was collected through centrifugation (at 5000 rpm, 10 min), washed sequentially with deionized water and ethanol to remove unbound ligand, and followed by drying at 70 °C for 12 h. The dry sample was used for experimental studies and for characterization. Fig. 1 shows the schematic diagram illustrates the preparation and functionalization of CM.

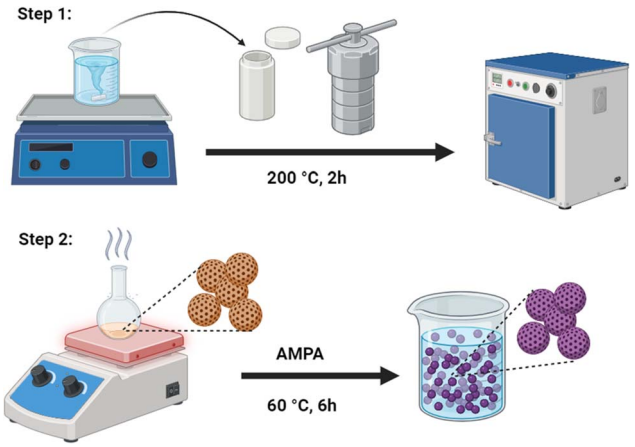

Fig. 1 Schematic illustration of FCM synthesis steps.

2.4. Characterization

The interferograms were acquired by collecting 32 scans, and the Fourier Transform Infrared (FT-IR) spectra were recorded using the PerkinElmer Spectrum Two spectrometer (Waltham, MA) using the KBr disk method in the 500–4000 cm^{-1} range at a resolution of 2.0 cm^{-1}. The JSM-7800F, JEOL microscope was used to capture images for the FESEM (field emission scanning electron microscopy), while the FEI-TECNIA G2 F30 S-TWIN transmission electron microscope, running at 300 kV, was used to record images for the HRTEM (high resolution transmission electron microscopy). The samples were mounted on a grid and then coated with gold. Using inductively coupled plasma optical emission spectroscopy (Avio 200, PerkinElmer), the amount of adsorbed metal ions was calculated. The porosity and surface area of the material were analyzed using a Brunauer–Emmett–Teller (BET) surface area analyzer (Thermo scientific, Surfer). The surface area and total pore volume for the nascent material were determined to be 127.6 $m^2\ g^{-1}$ and 8.2 $cm^3\ g^{-1}$, respectively, while those for the functionalized material were 123.5 $m^2\ g^{-1}$ and 5.7 $cm^3\ g^{-1}$, respectively. The incorporation of the ligand resulted in a slight decrease in both surface area and porosity, which can be attributed to the distribution of the ligand within the pores and on the surface of the material. This observation further supports the successful functionalization of the material.

2.5. Column procedure for trace metal separation

The studies were conducted using a glass column of 25 × 0.5 cm, which was equipped with a porous ceramic disk and a peristaltic pump. The column was first packed with 500 mg of functionalized carbon microspheres (FCM). A 100 mL sample solution with the ideal sample flow was passed through the column bed at optimum solution pH and with the suitable concentration of metal ions. After passing the sample the column was washed with deionized water to remove unabsorbed ions. Afterward, the optimized eluent with suitable volume was passed to elute the sorbed metal ions. The concentration of metal ions in the percolated solution was measured by ICP-OES.

3. Results and discussion

3.1. Characterization of FCM

The Fourier Transform Infrared (FT-IR) spectra of the functionalized composite material (FCM) are presented in Fig. 2. The spectrum reveals several key features indicative of functional groups present in the material. The peak observed at 3270 cm^{-1} corresponds to the stretching vibration of O–H groups, suggesting the presence of hydroxyl functionalities, which may enhance interactions with target analytes. Additionally, the stretching frequencies for aromatic C–H and C=C bonds are identified at 2900 cm^{-1} and 1230 cm^{-1}, respectively, indicating the retention of aromatic structures in the functionalized material. Furthermore, the peak at 1528 cm^{-1} is attributed to the stretching vibrations of C–N bonds, which implies successful incorporation of the ligand during the functionalization process. Collectively, these spectral features support the effective functionalization of the CM sorbent material with the ligand, enhancing its potential for specific analyte adsorption during application. The particle size analysis has been carried out using particle size analyzer after dispersing the particles in DI water. The average particle size for prepared material has been found to be 0.8 μm. Furthermore, the SEM image of prepared CM sorbent material presented in Fig. 3a and b, displays the surface morphology at different magnifications. It was observed that the obtained material has spherical shape with uniform distribution. Also, the TEM image (shown in Fig. 3c) observed after sonication in deionized water, they are well distributed into their single spherical form with good transparency. Fig. 3d–g displays the surface elemental mapping, which highlights the uniform distribution of elemental carbon, oxygen, nitrogen, and phosphorus originating from functionalized ligand and carbon microspheres. According to Fig. 3a–c, the morphology of CM as seen from different magnifications using SEM and TEM shows that the FCM are evenly distributed and have a porous structure that allows for smooth water flow during column studies. Additionally, the goniometer-measured data observed for water

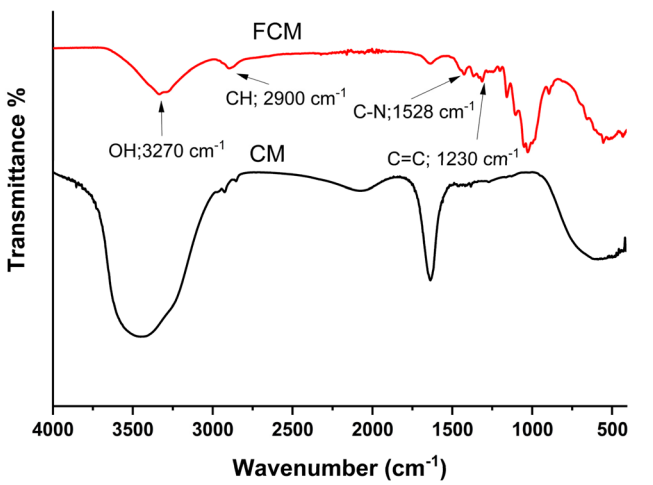

Fig. 2 FT-IR spectra of CM and FCM sorbent.

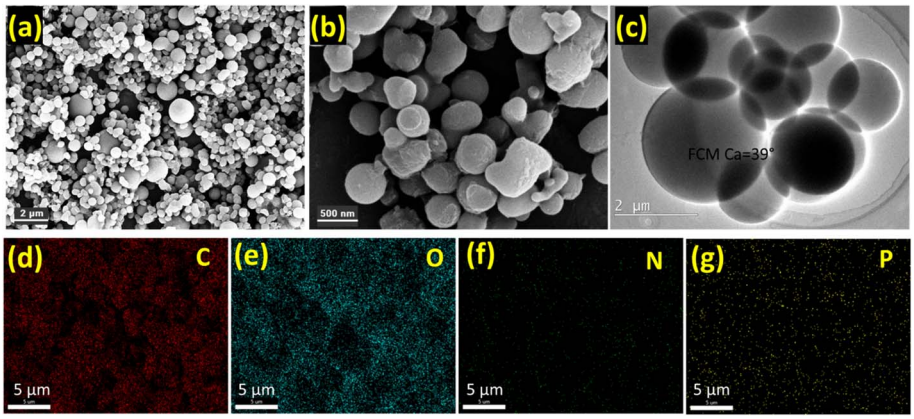

Fig. 3 (a and b) SEM micrographs of FCM at varying magnifications shows physical appearance with smooth surface morphology; (c) TEM micrographs of FCM depicts porous structure of FCM; (d–g) elemental mapping images of FCM depicts uniform distribution of constituent elements.

contact angle of the nascent CM observed at 60° decreased to 39° for FCM (Fig. 4), which is indicative of the enhanced hydrophilicity of FCM as a result of the functionalization of oxygen-containing ligand molecules and makes it more appropriate for aqueous sample analysis. Furthermore, after being stirred for 72 hours in distilled water, there was no discernible decrease in the sorption capacity of FCM were observed. This suggests that FCM is stable under water and can be utilized for repeated sample analysis in SPE.

3.2. Effect of sample pH

The adsorption behavior of the FCM towards Pb(II) and Cd(II) ions was systematically studied within a pH range of 3–7. To avoid metal precipitation, pH levels beyond 7 were not considered for the investigation. Buffer solutions, specifically HCl–$C_2H_5O_2N$, CH_3COOH–CH_3COONa, and Na_2HPO_4–$C_6H_8O_7$, were utilized to establish and maintain sample pH at 3.0–3.0, 4.0, 5.0, 6.0, and 7.0, respectively. To study the effect of solution pH on metal ion adsorption, a 100 mL sample solution containing 250 mg L^{-1} of Pb(II) and Cd(II) ions was adjusted to varying pH levels between 3.0 and 7.0 in an Erlenmeyer flask. After a 12 hours equilibration period with 0.5 g of FCM, the FCM material was centrifuged and collected, and the metal ion concentration in the effluent was determined using ICP-OES. Comparative analysis with nascent CM revealed a markedly enhanced adsorption efficiency of the FCM, attributed to robust soft–soft interactions between metal and functional groups (Fig. 5a and b). According to the HSAB theory, the predominant adsorption mechanism involved complex formation and electrostatic interactions, resulting in superior selectivity toward Pb(II) and Cd(II) within the pH range of 5.5–7.0 (Fig. 5b). Zeta potential analysis revealed a point of zero charge (pHz) at pH 4.8, signifying a negatively charged material surface that interacted favorably with positively charged metal ions. The more negative value of zeta potential corresponded to higher negative surface charges and increased heavy metal uptake. The zeta potential changed from −24.6 mV to 0.6 mV at an initial concentration of 250 mg L^{-1} of metal ions, equilibrated with FCM, suggesting surface adsorption of Pb(II) and Cd(II) ions. A more significant electrostatic attraction for metal ions towards the solid surface was suggested by lower zeta potential values. However, at a sample pH of 3.0, adsorption diminished due to protonation of functional groups, resulting in positive charges and reduced electrostatic interaction with metal ions. In contrast, as sample pH increased, deprotonation of functional groups induces a negative charge, fostering electrostatic attraction with positively charged metal ions at pH 5.0–7.0. Because nascent CM has fewer or less selective binding sites than FCM, it has a lesser capability for adsorbing Pb(II) and Cd(II). The pH range of 6.0–7.0 was shown to have the best adsorption of Pb(II) and Cd(II) ions (1.80 and 2.20 mmol g^{-1}), which led to the selection of pH 6.0 for further research.

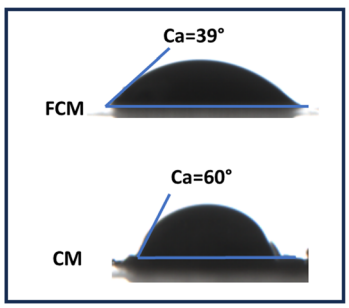

Fig. 4 Water contact measurement of FCM and CM depicts hydrophilicity of material.

3.3. Optimization of sample flow

To investigate the impact of sample flow on metal ions sorption, a series of experiments were conducted using a FCM packed column. For this, a 100 mL of individual sample solution with a pH of 6 and an initial Pb(II) and Cd(II) concentration of 250 mg L^{-1} were percolated through the column at varying flow rates ranging from 2 to 10 mL min^{-1}. The flow rate was precisely controlled using a peristaltic pump. Following the percolation and flushing the column with deionized water, the adsorbed

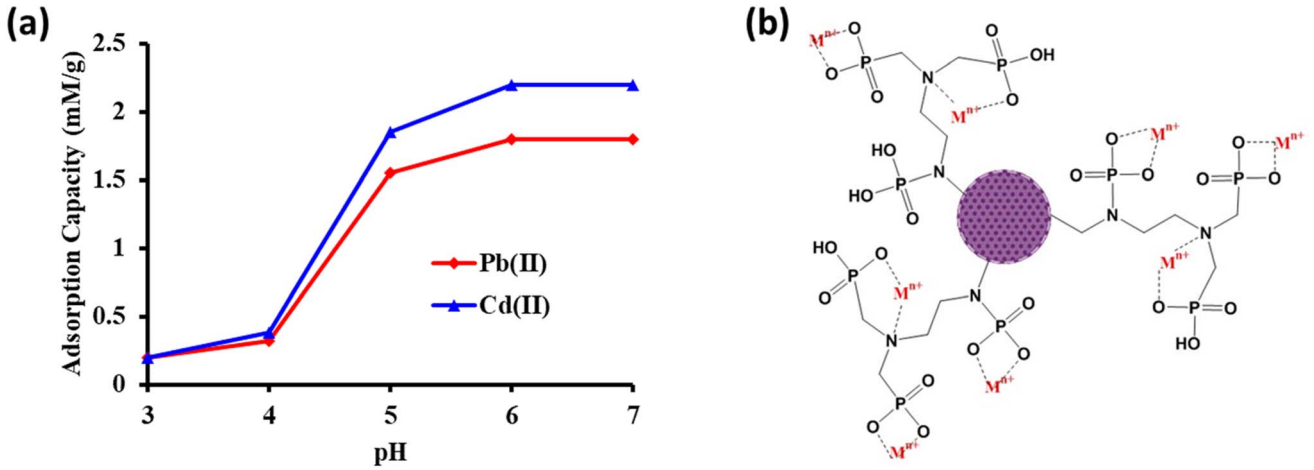

Fig. 5 (a) Effect of solution pH on the adsorption of metal ions (experimental condition: sample volume 100 mL; sorbent amount 500 mg; metal ion concentration 250 ppm; flow rate 8 mL min^{-1}); (b) possible adsorption mechanism of FCM by metal ion complexation at optimum sample pH.

metal ions were then eluted from the column, and their concentrations were quantified using ICP-OES.

The results, as illustrated in Fig. 6, revealed that the adsorption efficiency of FCM remained consistent up to a sample flow rate of 8.0 mL min^{-1}, indicating rapid kinetics and effective interaction between the sorbent and metal ions. However, as the sample flow rate in the column was increased beyond 8.0 mL min^{-1}, a gradual decline in the sorption efficiency was observed. At higher flow rates of 10 mL min^{-1}, the sorption efficiency decreased to 90% and 82% of total sorption capacity of Cd(II) and Pb(II), respectively. This decline in efficiency suggests that higher flow rates may result in insufficient contact time between the analyte and the binding sites on the sorbent, leading to reduced sorption.

In light of these findings, a sample flow rate of 8.0 mL min^{-1} was deemed optimal, balancing efficient sorption and practical considerations. This selected flow rate was subsequently applied to all further experiments. Similarly, the flow rate of the eluent, used to elute the retained metal ions from the column, was investigated. At an eluent flow rate of 2.0 mL min^{-1}, a remarkable recovery efficiency of 99.99% for Pb(II) and Cd(II) ions were achieved. This flow rate was deemed optimal for subsequent elution studies, ensuring effective recovery while maintaining experimental feasibility.

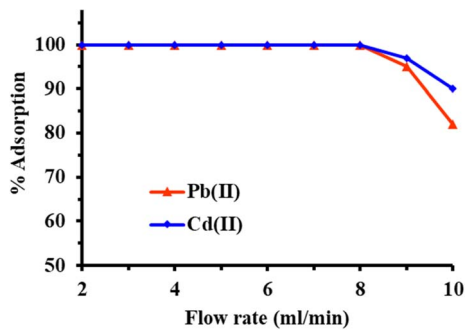

Fig. 6 Effect of solution flow rate on the adsorption of metal ions (experimental condition: sample volume 100 mL; sample pH 5.0; sorbent amount 500 mg; metal ion concentration 250 ppm).

3.4. Eluent suitability and reusability

Achieving high extraction efficacy and guaranteeing full recovery of the adsorbed analyte are key components of optimizing sorbent properties. A 100 mL metal ions solution (250 mg L^{-1}) percolated down the FCM packed column at a flow rate of 8.0 mL min^{-1} was used in this work to optimize the stripping agent. After that, the adsorbed metal ions were extracted from the column using different mineral acids, namely nitric and hydrochloric acid, at different concentrations (0.5–1.5 M) and volumes (2–5 mL).

The results, which are shown in Fig. 7, showed that elution with 5 mL of hydrochloric acid (0.5 M) produced a maximum recovery of 60%, while elution with nitric acid produced a recovery of 52% under the same circumstances. Complete recovery (>99.9% for hydrochloric acid and 95.0% for nitric acid) was noted after raising the eluent concentration to 1 M while maintaining an eluent volume of 5 mL. However, the recovery of metal ions was significantly reduced when the eluent volume was decreased to 3 mL at a constant concentration of 1 M. The ideal eluent was ultimately determined to be 5.0 mL of hydrochloric acid (1 M), which was utilized in the trials that followed.

The reusability of FCM sorbent has been analyzed by gradually passing a series of model solutions ($n = 50$, 100 mL each) containing 250 mg L^{-1} of metal ions through the column at a flow rate of 8.0 mL min^{-1}at multiple times, and the sorbed analyte after elution has been examined under ICP-OES. The recovery of metal ions in each eluent cycle is shown in Fig. 8. Analyte recovery over 96.0% was achieved by the FCM sorbent, which demonstrated effective reusability for up to 60 cycles. The adsorption of metal ions dropped to 80–85% after the 60 cycle, which can be related to the possibility of functional group loss

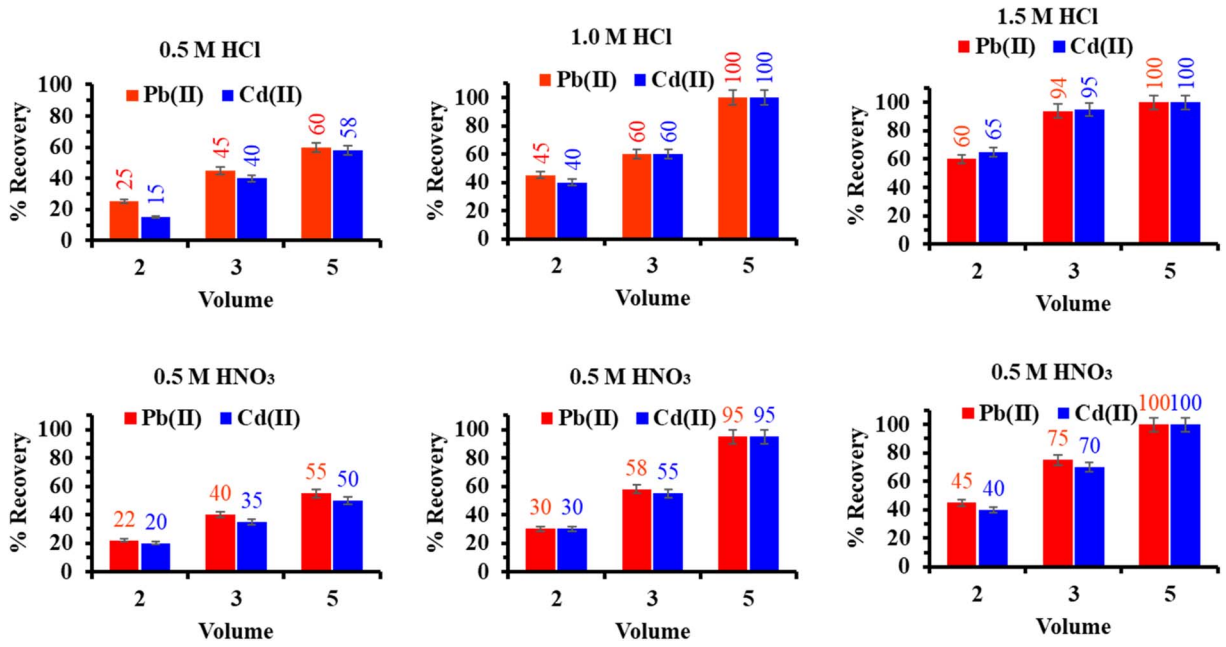

Fig. 7 Effect of different stripping agents (volume and concentration) on the recovery of adsorbed metal ions (experimental condition: sample volume 100 mL; sample pH 6.0; sorbent amount 500 mg; metal ion concentration 250 ppm; sample flow rate 8 mL min^{-1}).

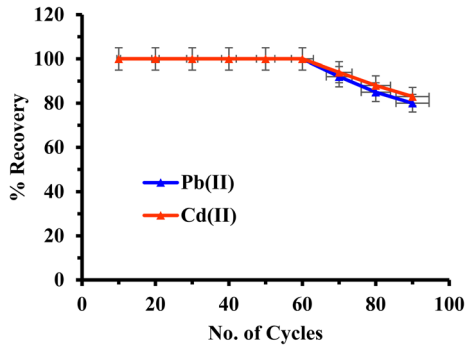

Fig. 8 Reusability of FCM for Pb(II) and Cd(II) extraction from aqueous solution (experimental condition: sample volume 100 mL; sample pH 6.0; sorbent amount 500 mg; metal ion concentration 250 ppm; flow rate 8 mL min^{-1}).

or degradation from repeated contact with the eluent (acid). The FCM packed column showed strong reusability in spite of this little decline, making it appropriate for several uses in actual sample analysis without sacrificing extraction performance.

3.5. Effect of coexisting ions

It is typical for mono-and/or divalent ions like Na, K, Ca, Mg, Cu, Co, Ni, Zn, Cr, Hg, and As to coexist with their co-anions in actual water samples. This coexistence makes extraction difficult and taints the process of identifying the target analytes. Generally speaking, cationic matrices vie with the analyte for the same sorbent binding sites, which reduces the target ion's capacity for sorption. When specific ions are later detected in real samples using ICP-OES, the co-existence of these ions frequently causes spectrum interferences.

In order to establish a tolerance limit, the interference effect resulting from co-existing ions was carefully examined in order to fully evaluate the sorption performance of the FCM in competing settings. A model solution of 100 milliliters, comprising 10 μg L^{-1} of Pb(II) and Cd(II) ions along with different concentrations of co-ions under investigation, was run through the FCM-packed column. For this, the primary objective was to determine the highest concentration of co-ions that induces significant interferences. Usually, the tolerance threshold was defined as the maximum stoichiometric ratio of interfering ions to the target analyte ions (Pb and Cd) that resulted in a change in analyte ion measurements of less than 5%. Herein, the results of the interference investigations are shown in Table 2, which shows an impressive 98–100% analyte

Table 2 Tolerance limit of co-existing ions on the extraction of Pb(II) and Cd(II) ions in binary mixture (experimental conditions: pH 6, total volume 100 mL; flow rate 8 mL min^{-1}, metal ions 100 μg L^{-1})

Added ions (salt used)	Tolerance ratio [added ions/metal ion]	Recovery (%)	RSD ($N = 3$)
Na^+ ($NaCl$)	4.0×10^3	98.5	3.5
K^+ (KCl)	3.5×10^4	98.0	4.0
NH_4^+ (NH_4Cl)	2.5×10^3	99.5	3.7
Ca^{2+} ($CaCl_2$)	4.5×10^2	97.5	4.0
Mg^{2+} ($MgCl_2$)	3.8×10^2	98.0	4.0
CH_3COO^- (CH_3COONa)	5.5×10^4	100.0	2.5
Cl^- ($NaCl$)	3.0×10^5	100.0	3.98
Br^- ($NaBr$)	4.5×10^6	100.0	3.5
SO_4^{2-} (Na_2SO_4)	4.5×10^5	98.0	3.6
CO_3^{2-} (Na_2CO_3)	5.5×10^5	100.0	3.8
NO_3^{2-} (Na_2NO_3)	4.5×10^5	99.0	2.5
Humic acid	150	97.0	3.5
Fulvic acid	150	99.2	3.7

recovery and no significant sorption and detection of Pb(II) and Cd(II) ions for the whole range of added ions. On the other hand, Pb(II) and Cd(II) ion adsorption shows a decline in sorption when the concentration of interferents ions increases beyond their threshold concentration ratio (Table 2). In optimal conditions, the quantitative recovery of Cd(II) and Pb(II) ions can be achieved, even in the presence of interfering species, as long as their concentration ratios remain within a specified acceptable range. This finding underscores the resilience and selectivity of the functionalized composite material (FCM) when analyzing complex water samples containing co-existing ions.

4. Preconcentration studies

The physical characteristics of the analyte composition and its trace concentration pose challenges in performing quantitative analyses, particularly when dealing with ions that are below the instrumentation's detection limit. Accurate and exact measurement of trace ions can be severely hampered by multiple factors such as presence of co-ions, poor instrumental detection limits, and close wavelength proximity of co-ions with analyte ions. Using a sample cleanup approach, the target analyte must be isolated from the complicated sample matrix in order to address this. Preconcentration is an analytical technique that isolates metal ions from an immense volume, even at trace amounts, and concentrates them into a small sample volume for accurate measurement. Determining the preconcentration factor, which is the ratio of these two volumes, is essential to assessing the process's effectiveness.

A bench of samples containing 1.0 μg of individual metal ions in various quantities (1200, 1600, 2000, 2300, 2500, 2700, and 3000 mL) was created for this study. The FCM column was used to filter these samples after the optimized process. Pb(II) and Cd(II) ions that had been adsorbed were then eluted and analyzed using ICP-OES. Up to a sample volume of 2500 mL, quantitative recovery of metal ions was accomplished. Beyond that, quantitative adsorption of Pb(II) and Cd dropped to 88% and 91%, respectively, with an increase to 2700 mL. The FCM sorbent was found to attain a preconcentration limit (PL = metal ions (μg)/volume of sample solution (L)) of 0.40 μg L^{-1}, which corresponds to an enrichment factor of 500. The FCM sorbent may be suitable for column usage in the measurement of trace metal ions, as shown by the high preconcentration limit. Pb(II) and Cd(II) ions can approach equilibrium in aqueous solutions more quickly thanks to the enhanced preconcentration efficiency and high density of surface functional groups of FCM. Additionally, with the proposed approach, the breakthrough studies has been conducted by passing a sample volume of 1500–5000 mL containing 1.0 mg L^{-1} of metal ions through the FCM packed column. The amounts of metal ions were assessed in effluent fractions that were sequentially collected. The breakthrough capacity (Pb-1.75 mmol g^{-1} and Cd-2.10 mmol g^{-1}) gets closer the maximum adsorption capacity for Pb(II) and Cd(II) (Pb-1.80 and Cd-2.20 mmol g^{-1}) attained in batch mode, according to the breakthrough curve shown in Fig. 9, indicating the beneficial use of the FCM sorbent in column techniques.

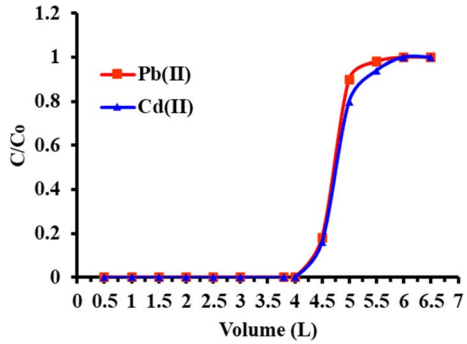

Fig. 9 Breakthrough profile of FCM for Pb(II) and Cd(II) adsorption (experimental condition: sample volume 100 mL; sample pH 6.0; sorbent amount 500 mg; metal ion concentration 250 ppm; flow rate 8 mL min^{-1}).

5. Analytical method validation

The created analytical method was put through a thorough testing process to assess its performance in terms of linearity, robustness, precision, accuracy, and detection limit, among other parameters. With a high R^2 value of 0.9998, the instrumental calibration that used the least square technique at six locations demonstrated linearity in the concentration range of 0–5000 μg L^{-1}. The accuracy of the procedure was evaluated by passing five replicate samples (each 100 mL) containing 5 μg of Pd(II) and Cd(II) ions at pH 6 through the column. This yielded five repeated measurements with a coefficient of variance of 2.45% and 3.68, respectively. As per the recommendations set forth by IUPAC, the detection limit (LOD) of the method was determined to be 0.04 μg L^{-1} by employing 3S m^{-1} standards for the mean blank signal across 20 typical samples. The mean concentration of metal ions analyzed by the developed approach was statistically insignificant compared to original values, even in the presence of additional concomitants, according to an evaluation of the approach's accuracy using Student's *t*-test values at the 95% confidence level. The standard addition method was used to evaluate the analytical method's reliability even more. The percentage recoveries varied from 99.3 to 100.5% for spiked amounts of analytes (2, 4 and 6 μg), with a low relative standard deviation (RSD) of less than 5%, indicating the accuracy and consistency of the approach. Changes were made to the ideal pH (6 ± 0.5) and sample flow (8 ± 0.5 mL min^{-1}) in order to assess the robustness of the suggested approach. Pb(II) and Cd(II) ions recovery continued to be high, surpassing 98.5%, in spite of these modifications, demonstrating the method's reliable operation in a varying circumstances.

6. Application: analysis of real samples

The efficacy of the prepared FCM sorbent for concentrating trace concentrations of Pb(II) and Cd(II) from diverse real samples, including fish (muscles), river water and tap water

Table 3 Analysis of real samples by proposed FCM packed column procedure (column parameters: pH 6.0, sample flow rate 8.0 mL min^{-1}, sample volume 500 mL; eluent volume 5.0 mL and eluent flow rate 2.0 mL min^{-1})

Samples	Amount added (μg)	Metal ion found (μg L^{-1}) ± standard deviation[a] (recovery percentage) Pb(II)	Cd(II)
Fish[c]	0	3.66 ± 0.05	4.50 ± 0.08
	2	5.62 ± 0.08 (99.0)	6.28 ± 0.07 (99.8)
	4	7.65 ± 0.15 (99.7)	8.28 ± 0.09 (99.8)
	6	9.65 ± 0.12 (99.9)	10.29 ± 0.12 (100.0)
River water	0	5.20 ± 0.15	3.60 ± 0.06
	2	7.19 ± 0.06 (99.9)	5.60 ± 0.17 (100.0)
	4	9.58 ± 0.08 (99.8)	7.58 ± 0.18 (99.6)
	6	11.20 ± 0.13 (100.0)	9.55 ± 0.32 (99.3)
Tap water	0	1.35 ± 0.04	nd[b]
	2	3.36 ± 0.06 (100.3)	2.02 ± 0.05 (100.5)
	4	5.30 ± 0.06 (100.5)	3.95 ± 0.18 (98.9)
	6	7.25 ± 0.06 (100.0)	6.0 ± 0.13 (100.1)

[a] Replicate = 3. [b] Not detected. [c] μg g^{-1}.

were investigated as a prelude to instrumental analysis. The results obtained from the analysis of real samples are presented in Table 3. Pb(II) and Cd(II) concentrations in fish, river and tap water samples were determined to be Pb-3.66, 5.2 and 1.35 ppb, and Cd-4.5 and 3.6 respectively, showcasing the sorbent's ability to enrich trace elements. The calculated enrichment factor for these samples were 100. To assess the reliability of the method in real sample analysis, the average percent recoveries of the spiked amount of analyte ranged from 99.0 to 99.9%, with a low relative standard deviation (RSD) of less than 5%. These results indicate the method's robustness and accuracy in determining Pb(II) and Cd(II) concentrations in complex real samples, underscoring its potential for environmental monitoring and analytical applications.

7. Conclusion

To address the preconcentration of trace metal ions in complex sample matrices, a novel solid-phase extraction (SPE) sorbent, FCM, was developed. Leveraging the hydrophilicity of ligand and the increased porosity achieved in CFM, this sorbent exhibited enhanced adsorption efficiency. The increased porosity facilitated the exposure of binding sites allowing for more efficient sorption. This structural design, with enhanced channels for water passage, contributed to an improved sorption capacity of the CFM sorbent. The effectiveness of the proposed approach was validated through the analysis of real samples with standard addition method, and its extended application to the cleanup of real samples. Additionally, the method was optimized to minimize sample volume while maximizing the concentration of trace analyte content. The achieved detection limit for the technique was determined to be 0.04 μg L^{-1}. The FCM composite packed column, proposed in this study, demonstrates its suitability for routine Pb(II) and Cd(II) analysis in food and water samples, showcasing its potential as an effective tool for environmental monitoring and analytical applications.

Data availability

All data used in this study were presented in the manuscript.

Conflicts of interest

The authors declare that they have no known competing financial interests.

Acknowledgements

The authors extend their thanks to Researchers Supporting Project (RSP2024R400), King Saud University (Riyadh, Saudi Arabia).

References

1 Z. Xu, Q. Zhang, X. Li and X. Huang, A critical review on chemical analysis of heavy metal complexes in water/wastewater and the mechanism of treatment methods, *Chem. Eng. J.*, 2022, **429**, 131688.
2 M. L. Sall, A. K. D. Diaw, D. Gningue-Sall, S. Efremova Aaron and J. J. Aaron, Toxic heavy metals: impact on the environment and human health, and treatment with conducting organic polymers, a review, *Environ. Sci. Pollut. Res. Int.*, 2020, **27**(24), 29927–29942.
3 C. S. Santana, D. M. Montalvan Olivares, V. H. C. Silva, F. H. M. Luzardo, F. G. Velasco and R. M. de Jesus, Assessment of water resources pollution associated with mining activity in a semi-arid region, *J. Environ. Manage.*, 2020, **273**, 111148.
4 J. Zhou, D. Obrist, A. Dastoor, M. Jiskra and A. Ryjkov, Vegetation uptake of mercury and impacts on global cycling, *Nat. Rev. Earth Environ.*, 2021, **2**(4), 269–284.
5 J. Wu, M. Cao, D. Tong, Z. Finkelstein and E. M. V. Hoek, A critical review of point-of-use drinking water treatment in the United States, *npj Clean Water*, 2021, **4**(1), 40.
6 Y. Palacios-Torres, J. D. de la Rosa and J. Olivero-Verbel, Trace elements in sediments and fish from Atrato River: an ecosystem with legal rights impacted by gold mining at the Colombian Pacific, *Environ. Pollut.*, 2020, **256**, 113290.
7 M. G. Uddin, S. Nash and A. I. Olbert, A review of water quality index models and their use for assessing surface water quality, *Ecol. Indic.*, 2021, **122**, 107218.
8 V. Panghal and R. Bhateria, A multivariate statistical approach for monitoring of groundwater quality: a case study of Beri block, Haryana, India, *Environ. Geochem. Health*, 2020, **43**, 2615–2629.
9 H. Ahmad, F. M. Husain and R. A. Khan, Graphene oxide lamellar membrane with enlarged inter-layer spacing for fast preconcentration and determination of trace metal ions, *RSC Adv.*, 2021, **11**(20), 11889–11899.

10 H. Ahmad, R. Ahmad Khan, B. Heun Koo and A. Alsalme, Cellulose Nanofibers@ZrO2 membrane for the separation of Hg(II) from aqueous media, *J. Phys. Chem. Solids*, 2022, **168**, 110812.

11 U. Haseen and H. Ahmad, Preconcentration and Determination of Trace Hg(II) Using a Cellulose Nanofiber Mat Functionalized with MoS_2 Nanosheets, *Ind. Eng. Chem. Res.*, 2020, **59**(7), 3198–3204.

12 H. Ahmad and C. Liu, Ultra-thin graphene oxide membrane deposited on highly porous anodized aluminum oxide surface for heavy metal ions preconcentration, *J. Hazard. Mater.*, 2021, **415**, 125661.

13 H. Ahmad, C. Cai and C. Liu, Separation and preconcentration of Pb(II) and Cd(II) from aqueous samples using hyperbranched polyethyleneimine-functionalized graphene oxide-immobilized polystyrene spherical adsorbents, *Microchem. J.*, 2019, **145**, 833–842.

14 L. Wang, X.-L. Wu, W.-H. Xu, X.-J. Huang, J.-H. Liu and A.-W. Xu, Stable Organic–Inorganic Hybrid of Polyaniline/α-Zirconium Phosphate for Efficient Removal of Organic Pollutants in Water Environment, *ACS Appl. Mater. Interfaces*, 2012, **4**(5), 2686–2692.

15 M. Yang, P. H. Li, S. H. Chen, X. Y. Xiao, X. H. Tang, C. H. Lin, X. J. Huang and W. Q. Liu, Nanometal Oxides with Special Surface Physicochemical Properties to Promote Electrochemical Detection of Heavy Metal Ions, *Small*, 2020, **16**(25), e2001035.

16 J. C. Xu, Q. Ma, C. Chen, Q. T. Wu and X. X. Long, Cadmium adsorption behavior of porous and reduced graphene oxide and its potential for promoting cadmium migration during soil electrokinetic remediation, *Chemosphere*, 2020, **259**, 127441.

17 H. Wang, L. Hou, Y. Shen, L. Huang, Y. He, W. Yang, T. Yuan, L. Jin, C. J. Tang and L. Zhang, Synthesis of core-shell UiO-66-poly(m-phenylenediamine) composites for removal of hexavalent chromium, *Environ. Sci. Pollut. Res. Int.*, 2020, **27**(4), 4115–4126.

18 T. Rasheed, A. A. Hassan, M. Bilal, T. Hussain and K. Rizwan, Metal-organic frameworks based adsorbents: A review from removal perspective of various environmental contaminants from wastewater, *Chemosphere*, 2020, **259**, 127369.

19 E. Yilmaz and G. Sarp, Graphene-like MoS2-modified magnetic C-dot nanoflowers: an efficient magnetic solid-phase extraction adsorbent for monitoring of trace amounts of ibuprofen, *Anal. Methods*, 2020, **12**(12), 1570–1578.

20 E. Yilmaz, S. Salem, G. Sarp, S. Aydin, K. Sahin, I. Korkmaz and D. Yuvali, TiO2 nanoparticles and C-Nanofibers modified magnetic Fe3O4 nanospheres (TiO2@Fe3O4@C-NF): A multifunctional hybrid material for magnetic solid-phase extraction of ibuprofen and photocatalytic degradation of drug molecules and azo dye, *Talanta*, 2020, **213**, 120813.

21 Y. Fang, L. Liu, H. Xiang, Y. Wang and X. Sun, Biomass-based carbon microspheres for removing heavy metals from the environment: a review, *Mater. Today Sustain.*, 2022, **18**, 100136.

22 A. Sanchez-Sanchez, F. L. Braghiroli, M. T. Izquierdo, J. Parmentier, A. Celzard and V. Fierro, Synthesis and properties of carbon microspheres based on tannin–sucrose mixtures treated in hydrothermal conditions, *Ind. Crops Prod.*, 2020, **154**, 112564.

23 H. Ahmad, R. A. Khan and A. Ali, Covalently linked mercaptoacetic acid on ZrO_2 coupled cellulose nanofibers for solid phase extraction of Hg(II): experimental and DFT studies, *RSC Adv.*, 2022, **12**, 35712–35721.

24 M. S. Rameetse, O. Aberefa and M. O. Daramola, Effect of Loading and Functionalization of Carbon Nanotube on the Performance of Blended Polysulfone/Polyethersulfone Membrane during Treatment of Wastewater Containing Phenol and Benzene, *Membranes*, 2020, **10**(3), 1–9.

25 A. Dongil, B. Bachiller-Baeza, A. Guerrero-Ruiz, I. Rodríguez-Ramos, A. Martínez-Alonso and J. Tascón, Surface chemical modifications induced on high surface area graphite and carbon nanofibers using different oxidation and functionalization treatments, *J. Colloid Interface Sci.*, 2011, **355**(1), 179–189.

26 N. Altunay, B. Hazer, M. Tuzen and A. Elik, A new analytical approach for preconcentration, separation and determination of Pb(II) and Cd(II) in real samples using a new adsorbent: Synthesis, characterization and application, *Food Chem.*, 2021, **359**, 129923.

27 D.-B. Zhou, H.-T. Zhu, Y.-Z. Hou, G.-L. Shen, C. Shi, Y.-J. Zhu, Y.-B. Xiao, W. Song, Y.-X. Liu, F. Han, P. Zheng and X.-F. Yu, Magnetic solid phase extraction for the determination of Pb(II) and Cd(II) in high salt foods, *J. Food Compos. Anal.*, 2024, **126**, 105921.

28 A. A. Gouda, R. El Sheikh, A. O. Youssef, N. Gouda, W. Gamil and H. A. Khadrajy, Preconcentration and separation of Cd(II), Co(II), Cu(II), Ni(II), and Pb(II) in environmental samples on cellulose nitrate membrane filter prior to their flame atomic absorption spectroscopy determinations, *Int. J. Environ. Anal. Chem.*, 2023, **103**(2), 364–377.

29 B. Feist, Dispersive Micro-Solid Phase Extraction Using a Graphene Oxide Nanosheet with Neocuproine and Batocuproine for the Preconcentration of Traces of Metal Ions in *Food Samples Molecules*, 2023.